Measurements of surface elasticity and thickness of 4′-*n*-octyl-4-cyanobiphenyl film at an air-water interface

Naoto Sakamoto, Keiji Sakai, and Kenshiro Takagi
Institute of Industrial Science, University of Tokyo, 7-22-1, Roppongi, Minato-ku, Tokyo 106, Japan
(Received 16 April 1997)

Two optical techniques, ripplon light scattering and convergent ellipsometry around the Brewster angle, were used to investigate the monolayer-trilayer phase transition in 8CB (4′-*n*-octyl-4-cyanobiphenyl) film expanded at the air-water interface. The former technique is useful to evaluate the surface elasticity of the film, while the latter estimates the film thickness from its reflectivity. These results were analyzed in correlation with the relevant Π-A isotherms. We showed that the elasticity of the monolayer film is 4×10^{-2} N m^{-1}, and that of the trilayer is 2×10^{-1} N m^{-1}, and that the latter is 2.0 times as thick as the former. Inhomogeneous structures in the coexistence of monolayer-trilayer phases, and the fluidity of the trilayer domains, were observed. Ripplon measurements were also made in the coexistence region of the monolayer and the gaseous phase. [S1063-651X(97)13608-X]

PACS number(s): 64.70.Md, 68.10.Et, 78.35.+c, 78.66.−w

INTRODUCTION

Structures of gas-liquid interfaces with a thin molecular film existing in between are of great interest, since they provide information about various kinds of molecular interactions. The interface supports many types of amphiphilic molecules which consist of a hydrophilic head and a hydrophobic tail. These molecules form monomolecular films at certain proper conditions. Each molecule turns up its hydrophobic tail into air, with its hydrophilic head down in water. Phase transitions of these monomolecular films have attracted considerable attention in recent years. The film is in a gaseous phase when the molecules are sparse enough, and more condensed phases appear as it is compressed. In typical fatty acid films, there are several phases which differ in density: gaseous, liquid expanded, liquid condensed, and solid like. In most cases the solid phase is the densest, and further compression often leads to a disordered collapse of the monolayer and the appearance of three-dimensional structures. The transition which occurs in the film of thermotropic liquid crystal 8CB (4′-*n*-octyl-4-cyanobiphenyl) is somewhat different [1–4]. When a monomolecular film of 8CB is excessively compressed in the plane, an ordered collapse occurs, and the monolayer is folded into a stable trilayer film, and the transition is believed to be of the first order. Xue, Jung, and Kim made an extensive study of Π-A isotherms by surface balance, where Π and A are the surface pressure and the surface area per molecule, respectively, and found this phenomenon [1]. They divided the whole range of A into five regions, from I through V, and concluded that the monolayer-trilayer phase transition occurs in region III (41 Å^2/molecule$>A>$12 Å^2/molecule) from the experimental results of both the ellipsometry and optical second-harmonic generation. Friedenberg *et al.* observed this region by Brewster angle microscopy (BAM), and visualized the coexistence of the monolayer and trilayer [2]. Mul and Mann also made a BAM investigation, and obtained a similar result [3]. The phase transition not between the monolayer and bilayer but between the monolayer and trilayer was supported by Schmitz and Gruler, who made a surface potential measurement in region III [4].

Recently we developed a technique of convergent ellipsometry around the Brewster angle (CEBA) for a quantitative evaluation of molecular films extended on an air-water interface [5]. This technique yields the angular dependence of the reflectivity of the interface, from which the film thickness is obtained. We have already applied this method to a stearic acid monomolecular film in the liquid phase, and made a quantitative discussion of its thickness. The usefulness of this technique has been shown. While this technique as well as the Π-A measurement gives the statics of the molecular film, the ripplon light scattering provides us with a dynamical approach to air-liquid interfaces. Ripplons are high-frequency capillary waves thermally excited on liquid surfaces and propagating with the surface tension as their major restoring force. Ripplon propagation is strongly affected by the structure at the surface and subsurface region. The dispersion relation of the waves reflects viscoelastic properties of the molecular film expanding itself at the interface. In our previous study, we established a system of hyper-resolution spectroscopy for ripplon light-scattering experiments [6]. We already applied this system for investigating relaxation phenomena of soluble films on liquid, the morphology and critical behavior of insoluble monomolecular films, and the sol-to-gel transition process of solutions [7–11].

A combination of the above two experimental techniques, CEBA and ripplon light scattering, would be effective in observing both statical and dynamical aspects of the phenomena in which the interface is involved: a more profound insight into the interfacial physics would be obtained. We therefore decided to apply the two techniques to an 8CB film on water. We also conducted a conventional Π-A measurement. The purpose of this study is to confirm the monolayer-to-trilayer phase transition from the viewpoints of film thickness and elasticity property. Though 8CB is one of the most widely used and studied materials of liquid crystals, the structure of the surface and subsurface is for the most part

left unknown. Molecular films at the air-water interface are important since they are regarded as a model of a skin of the bulk liquid crystal. The transition from the monolayer to the multilayer would reproduce the process of new-surface creation under an ideal condition. This is also one of our interests, lying in the background of this study.

EXPERIMENT

A ripplon experiment is a kind of dynamic light-scattering method for a liquid surface. A beam of an Ar^+ laser is incident on the liquid surface and scattered by the ripplon, whose wave number is determined by the scattering angle. Analysis of the scattered light by the optical beating technique yields the power spectrum of the light, from which the ripplon frequency and the damping are obtained. These two values give the two-dimensional elasticity and viscosity of the film. A more detailed description of the technique has been given elsewhere [6–10].

Principle and details of CEBA have already been given [5], and we offer only a brief account here. Incident light of a He-Ne laser with P polarization is once expanded to a beam with about 10-mm diameter, and then focused to a spot about 100 μm in diameter on the surface. The convergent incidence has the optical axis set roughly at θ_B, the Brewster angle of the substrate liquid, with the amplitude distribution almost uniform within $\pm 2°$ around θ_B. The divergent reflected light has a unique doughnutlike pattern with a dark hole in the center, if projected on a screen. A photodiode with a pinhole in its front is scanned in the direction of θ, the reflection angle, on the detection plane perpendicular to the reflection axis: the angular dependence of the reflectivity for the P-polarized light is obtained. Though the reflection perfectly vanishes at $\theta = \theta_B$ on a clean surface, a thin film on it causes a finite value of the minimum reflectivity, which gives the quantitative evaluation of the film.

The sample cell is a round trough made of glass 10 cm in diameter and 1 cm in depth. The same cell was used in all the three experiments: ripplon, CEBA, and Π-A. It was repeatedly rinsed by distilled water before use. We filled the cell with distilled water and floated a barrier made of a Teflon sheet 50 μm in thickness to determine the area in which molecules of the film were allowed to move. A solution in which 84 mg of 8CB was dissolved in 100 ml of hexane was dripped on the water surface inside the barrier with a microsyringe. The hexane evaporated quickly, leaving 8CB molecules which form a thin film. The amount of 8CB solution determines A.

8CB in its bulk state is a thermotropic liquid crystal which undergoes isotropic-nematic and nematic–smectic-A phase transitions at 40 and 33 °C, respectively. The film of 8CB, on the other hand, is reported to show no such transition in the temperature range from 10 to 38.7 °C [1]. The whole experiment was done at room temperature. The sample was purchased from Merck and used without further purification.

The surface pressure Π, which is determined as the decrease in surface tension due to the existence of a film, was measured as a function of A. We used the Whilhelmy method with a plate made of platinum. The Π-A isotherm was obtained by successive addition of 8CB on the surface. The result is shown in Fig. 1, which is almost the same as the previous results [1–4]. The surface pressure is required in obtaining elasticity in the ripplon measurement. We therefore measured Π around region II with special care.

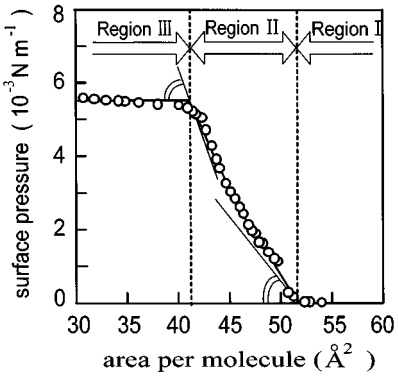

FIG. 1. Observed Π-A isotherm of 8CB film around region II. The surface elasticity of the monolayer is given by the gradient of this curve.

ELASTICITY OF THE FILM

The Π-A isotherm in Fig. 1 shows three distinct regions. In a dilute region at $A > 52$ Å^2/molecule, the surface pressure keeps a constant value at a very low level, indicating the coexistence of a condensed monolayer phase and a gaseous phase. At $A \sim 52$ Å^2/molecule, the surface is expected to be entirely covered with the condensed monolayer film. Further addition of the molecules causes a monotonous increase in the pressure up to $\Pi = 5.5 \times 10^{-3}$ N m^{-1}. The uniform film of the condensed phase is elastically compressed in this region II. The pressure reaches a plateau at $A = 41$ Å^2/molecule: the monolayer can no longer exist stably, and the ordered collapse begins. The trilayer domains appear in the monolayer phase. The almost constant value of Π in this stage indicates the first-order phase transition.

The above is an explanation of the isotherm given in terms of the phase transition between gas, monolayer, and trilayer. The ripplon study should be done so that its results are correlated with this Π-A curve. First we made a measurement in region I, the coexisting region of the gas and the condensed monolayer. We made this preliminary experiment in order to test the validity of the ripplon light scattering applied to the system of 8CB films. Figure 2 shows the results obtained at $A = 83$ Å^2/molecule, the coexistence state of the gaseous and the condensed monolayer phase. For this experiment, we used a floating Teflon sheet with a special shape which loosely divided the surface of measurement into two areas, one being exclusively covered with the condensed phase while the other with the coexisting gas. The two areas are connected through a narrow channel. Thus we can make the light-scattering experiment selectively in either phase. The shape of the Teflon sheet has already been given in detail elsewhere [10]. The ripplon frequency ω and the damping Γ are pointed on a chart which gives the two-dimensional elasticity ε and viscosity κ of a film covering the surface of ripplon propagation. The solid lines are the theoretical curves of constant viscosity along which ε increases anticlockwise. The outmost curve is for $\kappa = 0$, and κ increases as the curve shrinks. This set of curves is for Π

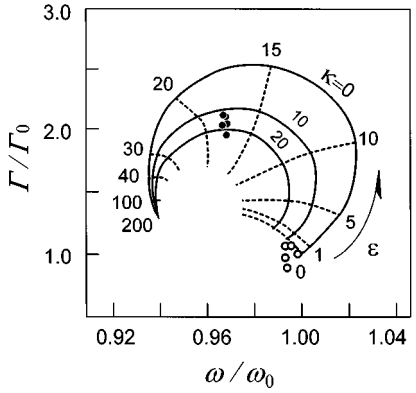

FIG. 2. The chart used to determine the surface elasticity ε and the surface viscosity κ from the ripplon spectra. The abscissa and the ordinate are the ripplon frequency ω and the damping Γ, normalized with respect to values for the water surface with virtual nonviscoelastic film whose surface pressure is $\Pi = 1.0 \times 10^{-4}$ N m^{-1}. The open and closed circles indicate the values for the gaseous phase and the monolayer, respectively, and the figures for ε and κ are given in the unit of 10^{-3} N m^{-1} and 10^{-9} kg s^{-1}, respectively.

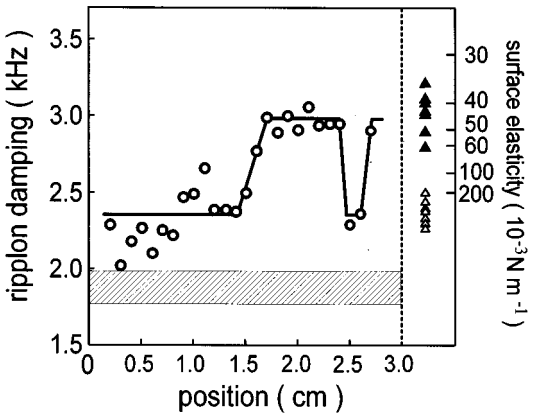

FIG. 3. Ripplon damping observed by the scanning ripplon measurement on the surface at the coexistence state of the monolayer and trilayer. The higher value corresponds to the monolayer phase, and the lower to the trilayer. The hatched belt shows the typical scatter in the damping for the clean water surface observed in a similar experiment. The damping is converted into the elasticity, which is represented by the right-hand ordinate. The closed and open triangles show the elasticity for the presumable monolayer and trilayer, respectively.

$= 1.0 \times 10^{-4}$ N m^{-1} in region I. The open and closed circles indicate the results obtained at the gas and at the condensed areas, respectively. These results tell us that the condensed phase has surface elasticity, $\varepsilon = 1.7 \times 10^{-2}$ N m^{-1}, and a finite value of surface viscosity, and the gas phase shows no observable elasticity. The elasticity of the coexisting condensed phase appears in the Π-A curve of Fig. 1 as the gradient at the dilute end of region II. We can calculate the elasticity of the monolayer, ε_M, by

$$\varepsilon_M = -A_0 \left(\frac{d\Pi}{dA} \right)_{A \to A_0}, \tag{1}$$

where A_0 is the area at the boundary between regions I and II. We obtained $\varepsilon_M = 1.8 \times 10^{-2}$ N m^{-1} with $A_0 = 51.6$ Å^2/molecule. This value is in good agreement with the one determined by the above ripplon measurement.

The gradient increases with decreasing A in region II, indicating that the film has a strong nonlinear nature in elasticity. The elasticity is determined to be $\varepsilon_M = 3.3 \times 10^{-2}$ N m^{-1} from Eq. (1), with $A_0 = 41.2$ Å^2/molecule, which is the dense end of region II. This is the elasticity of the monolayer film under coexistence with the trilayer film, and to be compared with the result of the ripplon experiment made in region III.

Figure 3 shows the results of scanning ripplon measurement made at $A = 14.6$ Å^2/molecule in region III, where the trilayer film is expected to cover $\sim 50\%$ of the whole area inside the Teflon barrier. This time the barrier was a simple circular shape. The light-scattering experiments were carried out in a spatial scan at every 1 mm along the x axis on the surface. The open circles in the figure represent the ripplon damping at each position. The scattering angle was fixed at 0.38°, which gives the ripplon wave number $k = 8.4 \times 10^4$ m^{-1}. There appear two weakly stable regions in this scan: one at $x \cong 0.5$ cm with $\Gamma < 2.5$ kHz, and the other at $1.5 \lesssim x \lesssim 2.5$ cm with $\Gamma \cong 3.0$ kHz, though the difference is less than conspicuous. The hatched belt in Fig. 3 indicates the result of a similar experiment made on a clean water surface, and shows that scatter in the data is within 200 Hz if there is no structure on the surface. The fluctuation in Γ observed in 8CB film is nontrivial and meaningful enough, reflecting the structure on the surface.

The morphological study by BAM reveals that the trilayer phase forms domains about 500 μm in diameter surrounded by the monolayer [3]. Although the spatial resolution of the scanning ripplon study is ~ 1 mm and not sufficient to reproduce the fine structure of the trilayer-monolayer coexistence, we can at least conclude that Γ shows a bistable fluctuation between two values, 3.0 kHz and below 2.5 kHz. The next step is to convert the change of Γ into that of ε. We need an ω-Γ chart like that of Fig. 2, but for $\Pi = 5.5 \times 10^{-3}$ N m^{-1}, the surface pressure in region III. As mentioned above, the point (ω,Γ) traces the horseshoe-shaped curve anticlockwise with increasing ε. When the film is very soft, i.e., $\varepsilon \leqslant 1.5 \times 10^{-2}$ N m^{-1}, the point moves up the right leg of the horseshoe as ε increases. The increase is sensitively observable as the increase in Γ. At the top of the horseshoe, on the other hand, ω is more sensitive to ε than Γ. In the experiment made in the monolayer-gas coexistence, the difference in ε is in the range where both ω and Γ vary with ε: the film strongly affects the ripplon propagation. Unfortunately, ε of both films in the monolayer-trilayer coexistence is in a range larger than 3.0×10^{-2} N m^{-1}, the range where many points of (ω,Γ) gather at the foot of the left leg in the chart. The films are too hard to affect the ripplon propagation anymore, and Γ alone is weakly sensitive to ε. The ordinate for ε thus determined by the chart is shown on the right-hand side of Fig. 3. The axis is inversely directed and far from linear. Nevertheless, we can deduce from this result that a very hard film with $\varepsilon \gtrsim 2 \times 10^{-1}$ N m^{-1} exists at $0.2 < x < 1.4$ cm and at $2.5 < x < 2.6$ cm, and that there is another film with $\varepsilon \cong 4.5 \times 10^{-2}$ N m^{-1} at $1.7 < x < 2.5$ cm on this surface.

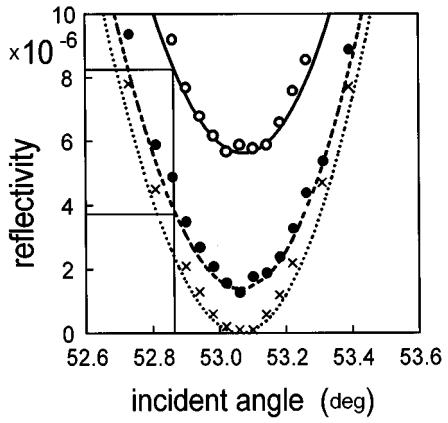

FIG. 4. The reflectivity curves obtained by CEBA, of which the open circles, the closed circles, and the crosses indicate the result for the surface at $A=12.5$ Å^2/molecule, at $A=39.9$ Å^2/molecule, and the clean water surface, respectively. The solid and dashed lines are the theoretical curves of Eq. (2) fitted to the points, while the dotted line is the theoretical curve for a clean water surface. The vertical straight line indicate the angle at which the measurement of Fig. 6 was done.

It would be quite natural to assign the soft and hard films to the monolayer and the trilayer, respectively. To verify this assumption, we made a ripplon study in the same sense as that of Fig. 2. The specially shaped Teflon barrier was used again. The surface under study was loosely divided into two areas, one likely to be covered with a monolayer, the other with a trilayer, and measurements were done at either area. The closed and open triangles on the right-hand side of Fig. 3 represent the elasticity observed at the presumable monolayer and trilayer areas, respectively. These points indicate that $\varepsilon_M \cong 4.0\times10^{-2}$ N m^{-1} and $\varepsilon_T \gtrsim 2\times10^{-1}$ N m^{-1}, where subscript T is the value for the trilayer. Note that ε_M and ε_T are in good agreement, respectively, with the lower and higher levels of the elasticity observed in the scanning ripplon measurement, and that ε_M agrees well with the static value $\varepsilon_M \cong 3.3\times10^{-2}$ N m^{-1} obtained from Π-A curve in Fig. 1. It would be quite reasonable to associate the very hard area and the softer area found by the scanning ripplon study with the trilayer and monolayer, respectively. The large scatter in the trilayer region would reflect the fine structure visualized by the BAM study; the area $0.2<x<1.4$ cm would be a trilayer-domain-rich region.

THICKNESS OF THE FILM

The advantage of CEBA is in its ability to evaluate the thickness of films on a liquid surface. Expecting to detect the difference in the thickness, we applied this technique to the monolayer-trilayer system. We also measured the clean water surface to check the reliability of the experiment. The crosses in Fig. 4 show the reflectivity of the virgin surface before 8CB film is expanded. If the initial surface is clean and the CEBA system is working correctly, the reflection of P-polarized light completely vanishes at θ_B which is determined by the index of refraction for water. The minimum reflectivity observed is zero within the experimental accuracy, and this angle should be θ_B for water. The point $\theta_B = 53.06°$ on the abscissa of Fig. 4 was thus fixed, and the scale was determined by the displacement of the pinhole on the detection plane and the focal length of the collimating lens. The dotted line is the reflectivity curve of a well-known theory [12], which is in very good agreement with the experimental points in this angular range.

After floating a circular-shaped barrier, an appropriate amount of 8CB molecules was dripped on this surface, and the area was adjusted to $A=39.9$ Å^2/molecule, near the boundary between regions II and III where the monolayer of the most compressed state extends over almost the whole surface. The reflectivity observed is shown by the closed circles in Fig. 4. The existence of the monolayer increases the reflectivity almost uniformly over this angular range without a significant change in the curve shape and the angle of minimum reflection, the latter implying that the film has no optical absorption. Then the molecules are added again to $A=12.5$ Å^2/molecule, at which the surface is fully covered with the trilayer film. The CEBA measurement was done to derive the result, as shown by the open circles in Fig. 4. The trilayer film increases the reflectivity in a similar manner but in a larger magnitude.

The theoretical curve of reflectivity to be correlated with the CEBA experiment is given by a pure geometrical optics. When a thin transparent film exists on a water surface to compose an air-film-water system with two interfaces, the reflectivity of P-polarized light is expressed as

$$R_P(\theta)=\frac{r_0^2+r_1^2+2r_0r_1\cos2\delta}{1+r_0^2r_1^2+2r_0r_1\cos2\delta}, \tag{2}$$

$$\delta=\frac{2\pi}{\lambda}nh\cos\xi, \tag{3}$$

where r_0 and r_1 are Fresnel coefficients of air-film and film-water interfaces, respectively, n and h are the refractive index and thickness of the film, respectively, ξ is the angle of incidence from the film to the water, and λ is the wavelength of the probe laser light [12]. Though θ is absent here in an explicit form, ξ is related to θ through Snell's law, and r_0 and r_1 are given as functions of n. Thus this equation includes two independent parameters n and h, and the best fit of this theoretical curve to the experimental data over a certain angular range would determine both n and h, if the fitting is precisely made. Unfortunately, the contributions of n and h to the shape of the curve are made mostly through nh. While the minimum reflectivity determines nh very accurately, the whole fitting is hopelessly sensitive to individual n or h. In the absence of any reliable value of n for molecular films of 8CB, we decided to make the curve fitting so that it gives h as a function of n over some proper range. The dashed and solid lines in Fig. 4 represent examples of the curves of Eq. (2) fitted to the reflectivity of monolayer and trilayer, respectively. In these fittings, $n=1.55$ was assumed for both films, and $h_M=1.07$ nm for the monolayer and $h_T=2.15$ nm for the trilayer were determined. In this way we obtained $h_M(n)$ and $h_T(n)$ as shown by the dashed and solid curves in Fig. 5, respectively. The range of the abscissa in the figure was chosen from the following considerations. Nematogen molecules generally have an anisotropic index of refraction in their nematic phase. In nCB's, they are known to be about 1.7 in the crystal axis and about 1.5 in the

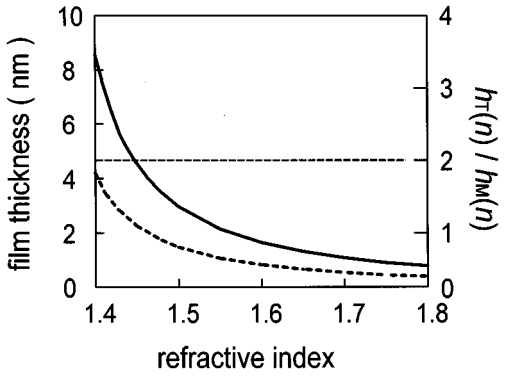

FIG. 5. Thickness of the trilayer (solid line) and monolayer (dashed) determined in the fitting of Eq. (2) to the experimental results shown in Fig. 4, and given as functions of the refractive index. The thin horizontal dashed line is the ratio h_T/h_M at each refractive index.

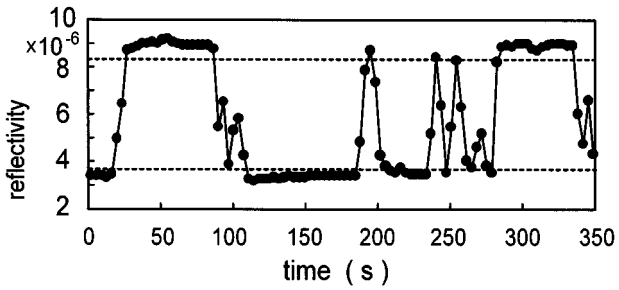

FIG. 6. The reflectivity observed for 6 min at a certain fixed spot on the film at the coexistence state ($A=18.3$ Å^2/molecule). The data show an obvious bistable change between the two horizontal lines, which correspond to the reflectivity of the trilayer and monolayer for the observation angle indicated in Fig. 4.

perpendicular direction. The effective value of n for a certain angle of incidence is given by the index ellipsoid and somewhere between the two values, $1.5<n<1.7$, would be a practical range.

The thickness of the monolayer $h_M=1.07$ nm at $n=1.55$ would be quite reasonable, consistent with a rough estimation made from the molecular structure. Note, however, that our primary interest is not in the absolute value of h_T or h_M, but in the ratio of the former to the latter. The thin horizontal dashed line in Fig. 5 represents the experimental value of h_T/h_M, which is neatly at 2.0 within 5% precision throughout this range. The above result of $h_T(n)/h_M(n)=2.0$ is in very good agreement with Xue, Jung, and Kim's experiment of ellipsometry which gave $h_T/h_M=2.12$ [1]. Both results are, however, against the simplest model of a trilayer which predicts $h_T/h_M=3$, and seemingly suggest a monolayer-bilayer transition. Nevertheless, previous studies, as well as ours, are on the standpoint for the hypothesis of the trilayer. The major reason for this is that the molecular density on the surface is about 3.5 times larger at the dense end of region III than at its dilute end, while a simple doubling of the monolayer suggests it is only twice as large. A commonly accepted model of the trilayer is that the compression of the monolayer buckles the film upward to form a bilayer in which the hydrophilic cores of 8CB are interdigitated inside, and the bilayer is folded over the monolayer so that the two hydrophobic surfaces contact face to face. Hence the top surface of the trilayer is also hydrophobic, as was suggested by the surface potential experiment of Schmitz and Gruler [4]. The interdigital structure of the bilayer would reduce the total thickness, and this is the reason why h_T/h_M is less than 3.

In the estimation of h_T/h_M made in Fig. 5, we assume that the trilayer has the same refractive index as the monolayer. Though this assumption is valid in the simplest model of the trilayer, it loses ground in the above model of a bilayer over the monolayer. The thin bilayer film of interdigitated structure implies a closer packing of molecules than the monolayer film, and hence a higher index of refraction. If this is true and the average index of refraction is increased in the trilayer, then the analysis in Fig. 5 should be corrected to give $h_T(n)/h_M(n)<2.0$. The bilayer could be even thinner than the monolayer, though a quantitative estimation is very difficult.

The closer packing in the bilayer is also suggested by the ratio of A values at both ends of region III. The ratio is about 3.5 as given above, which may mean that the bilayer has more molecules per unit area than twice the monolayer does. The molecules in the monolayer are bound to the surface, whose hydrophilic core is fully or partially in water and whose hydrophobic tail is in air at a certain tilt angle. The range of A in region II indicates that the area occupied by one molecule of the monolayer is a square whose side is 6.4–7.2 Å, reasonable values if the core size is taken into account. The major force that forms this structure of the monolayer is the strong interaction of each molecule with water, together with the effect of the exclusive area. On the other hand, the major force forming the bilayer structure is the coupling between two molecules. It is known that 8CB molecules tend to form pairs. An excess compression of the monolayer would release some molecules from the bondage of water, and two of them immediately make a side-by-side pair pointing oppositely. This pairing occurs successively, and the ordered bilayer in which the molecules align alternately is formed. The fact that h_T/h_M can be even smaller than 2 implies a firmly interdigitated structure with a large tilt angle of the pairs.

The bilayer and monolayer share a hydrophobic-hydrophobic interface where a weak frictional interaction probably governs. The bilayer film would smoothly slide on the monolayer. Figure 6 shows the temporal fluctuation of the reflectivity observed for 6 min by CEBA in region III, $A=18.3$ Å/molecule. The laser spot was fixed at one point on the surface of trilayer-monolayer coexistence, and the observation angle is slightly off the minimum, as indicated by the vertical line in Fig. 4. The reflectivity R shows a flipflop change between 8.3×10^{-6} and 3.7×10^{-6}, which correspond to the intersects of the straight line with the curves for the trilayer and monolayer in Fig. 4, respectively. In the period $25<t<90$ s, for instance, the laser happens to illuminate the trilayer domain: R is at the upper level. Then the domain slides away and R falls down to the lower level. From the transition time between the two levels together with the laser spot size, one can roughly estimate speed of the domain drift, $\sim10^{-5}$ m s^{-1}. Further, this speed and the typical period of the upper level, $\sim10^2$ s, roughly give the domain size $\sim10^{-3}$ m. This size is consistent with the result

of the observation by BAM [3]. The fluidity of the trilayer domain was also observed by other researchers [2,3].

In summary, we characterized the coexisting trilayer and monolayer of 8CB on a water surface by elasticity and thickness measurements. The results, together with the knowledge obtained so far, disproved the possibility of a simple trilayer with threefold monolayers, and suggested a structure of a bilayer placed on the monolayer. The monolayer is formed by the strong interaction of the hydrophilic core of an individual molecule with the substrate water. Each molecule is anchored and forced to stand up with a certain tilt angle of the hydrophobic tail. The average separation between the neighbors in the monolayer can be slightly expanded due to a repulsive force possible between the two molecules oriented in the same direction. In the bilayer film, on the other hand, molecules are alternately ordered by the close coupling between the inversely oriented molecules, and form a layer of tightly interdigitated structure. The tilt angle of the composing molecules is determined not by the interaction with the monolayer below but by the coupling geometry of the molecules within the film. The upper bilayer can glide freely over the hydrophobic face of the monolayer, since there is no strong interaction in between.

The bilayer of such a structure can be associated with a hard film with a high elasticity. The simplest model for the trilayer elasticity is a parallel connection of three springs with the same spring constant, which predicts $\varepsilon_T/\varepsilon_M=3$. In the present measurement of elasticity, we obtained $\varepsilon_M \cong 4\times10^{-2}$ N m^{-1} and $\varepsilon_T \gtrsim 2\times10^{-1}$ N m^{-1}, giving $\varepsilon_T/\varepsilon_M \gtrsim 5$, though ε_T of 8CB is in the range where the ripplon measurement loses a sufficient accuracy.

ACKNOWLEDGMENT

This work was supported partly by a Grant-in-Aid from the Ministry of Education, Science, Sports, and Culture.

[1] J. Xue, C. S. Jung, and M. W. Kim, Phys. Rev. Lett. **69**, 474 (1992).
[2] M. C. Friedenberg, C. G. Fuller, C. W. Frank, and C. R. Robertson, Langmuir **10**, 1251 (1994).
[3] M. N. G. de Mul and J. A. Mann, Jr., Langmuir **10**, 2311 (1994).
[4] P. Schmitz and H. Gruler, Europhys. Lett. **29**, 451 (1995).
[5] M. Hosoda, H. Kobayashi, N. Sakamoto, K. Sakai, and K. Takagi, Rev. Sci. Instrum. **67**, 4224 (1996).
[6] K. Sakai, P.-K. Choi, H. Tanaka, and K. Takagi, Rev. Sci. Instrum. **62**, 1192 (1991).
[7] K. Sakai and K. Takagi, Langmuir **10**, 257 (1994).
[8] K. Sakai and K. Takagi, Langmuir **10**, 802 (1994).
[9] T. Tokui, N. Sakamoto, K. Sakai, and K. Takagi, Jpn. J. Appl. Phys. **34**, L1682 (1995).
[10] N. Sakamoto, K. Sakai, and K. Takagi, Phys. Rev. E **53**, 6164 (1996).
[11] H. Kikuchi, K. Sakai, and K. Takagi, Phys. Rev. B **49**, 3061 (1994).
[12] M. Born and E. Wolf, *Principles of Optics*, 2nd ed. (Pergamon, Oxford, 1964), Chap. 7, p. 324.